ANATOMIA HISTOLOGIA EMBRYOLOGIA
JOURNAL OF VETERINARY MEDICINE

Anatomia, Histologia, Embryologia

ORIGINAL ARTICLE

Computed Tomography of the Normal Bovine Tarsus

U. Hagag[1,2]*, M. Tawfiek[3], W. Brehm[1] and K. Gerlach[1]

Addresses of authors: [1] Large Animal Clinic for Surgery, Leipzig University, An den Tierkliniken 21, Leipzig 04103, Germany;
[2] Faculty of Veterinary Medicine, Department of Surgery, Anesthesiology and Radiology, Beni-Suef University, Beni-Suef 62511, Egypt;
[3] Faculty of Veterinary Medicine, Department of Anatomy and Embryology, Beni-Suef University, Beni-Suef 62511, Egypt

***Correspondence:**
Tel./fax: 00 20 822 327982;
e-mail: usamahagag@yahoo.de

With 11 figures

Received August 2015; accepted for publication April 2016

doi: 10.1111/ahe.12233

Summary

The objective of this study was to provide a detailed multiplanar computed tomographic (CT) anatomic reference for the bovine tarsus. The tarsal regions from twelve healthy adult cow cadavers were scanned in both soft and bone windows via a 16-slice multidetector CT scanner. Tarsi were frozen at -20° C and sectioned to 10-mm-thick slices in transverse, dorsal and sagittal planes respecting the imaging protocol. The frozen sections were cleaned and then photographed. Anatomic structures were identified, labelled and compared with the corresponding CT images. The sagittal plane was indispensable for evaluation of bone contours, the dorsal plane was valuable in examination of the collateral ligaments, and both were beneficial for assessment of the tarsal joint articulations. CT images allowed excellent delineation between the cortex and medulla of bones, and the trabecular structure was clearly depicted. The tarsal soft tissues showed variable shades of grey, and the synovial fluid was the lowest attenuated structure. This study provided full assessment of the clinically relevant anatomic structures of the bovine tarsal joint. This technique may be of value when results from other diagnostic imaging techniques are indecisive. Images presented in this study should serve as a basic CT reference and assist in the interpretation of various bovine tarsal pathology.

Introduction

The bovine tarsus is a composite joint that comprises many joints, ligaments and tendons (Budras et al., 2011). Therefore, it is considered an important source of lameness in the hindlimb of cattle (Nelson and Kneller, 1985). Bovine lameness is one of the greatest constraints to productivity, health and welfare causing significant losses to animal breeders (Hernandez et al., 2002). Early detection of pathologic changes helps in determination of prognosis and clinical benefit of treatments (Blaik et al., 2000). Currently, radiography and ultrasonography are used to evaluate a wide range of orthopaedic problems in cattle (Kofler et al., 2014). Indecisive outcomes obtained via these techniques create the necessity for a cross-sectional imaging modality such as CT (Tomlinson et al., 2003). The advantages of CT include depiction of detailed cross-sectional anatomy without distraction from superimposed structures, improved contrast resolution, quantification of tissue physical densities, computer reconstruction of multiplanar images and consequently enhanced joint and bone qualification (Raes et al., 2011).

Currently, CT enjoys a prominent role in the diagnosis and evaluation of many bovine diseases (Nuss et al., 2011). An ever-increasing number of clinical reports involving CT assessment of bovine diseases are appearing in literature (Frame et al., 2000; Van Biervliet et al., 2004; El-Khodery et al., 2008; Frederick et al., 2009; Becker et al., 2011; Lee et al., 2011). Because of the complexity of the bovine tarsus, a CT anatomy guide with standard reconstruction planes is necessary for accurate interpretation of CT images in patients. CT anatomy of the tarsus has been studied in the horse (Tomlinson et al., 2003; Raes et al., 2011), the dog (Gielen et al., 2001) and the dromedary camel (Hagag et al., 2013) but until now, a reference for the normal CT anatomy of the bovine tarsus has not been published. Therefore, the purpose of this study was to provide a detailed multiplanar CT reference

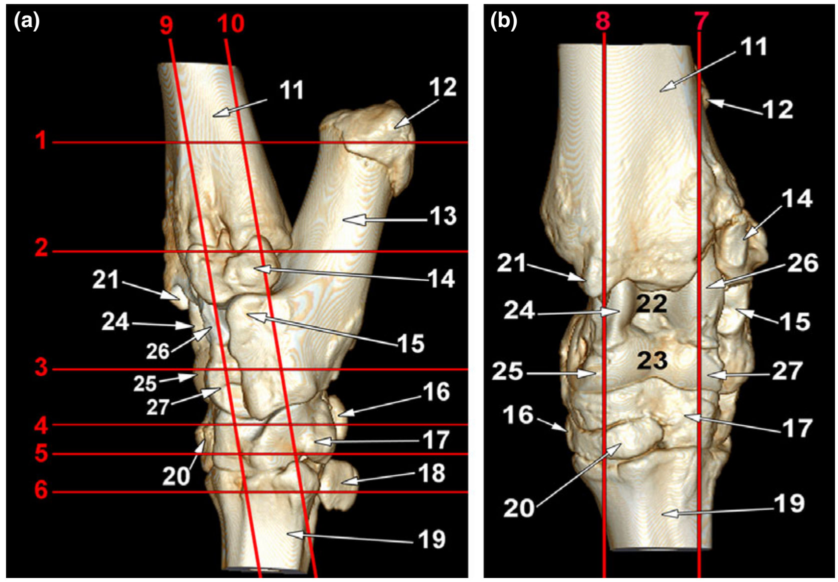

Fig. 1. Three dimensional CT reconstructed views of the normal bovine tarsus. Numbered red lines indicate the approximate levels of each anatomic slice of the frozen cadaver and the two corresponding contiguous computed tomographic images: a— Lateroplantar view showing the selected planes for the transverse CT levels (1–6) and dorsal CT levels (9–10), b— Dorsal view showing the selected planes for the sagittal CT levels (7–8): (11) Tibia; (12) Calcaneal tuber; (13) Calcaneus; (14) Malleolar bone; (15) Coracoid process; (16) 1st tarsal bone; (17) Centroquartal bone; (18) Sesamoid metatarsal bone; (19) 3rd and 4th metatarsal bones; (20) Fused 2nd and 3rd tarsal bones; (21) Medial malleolus; (22) Proximal trochlea of the talus; (23) Distal trochlea of the talus; (24) Medial ridge of the proximal trochlea of the talus; (25) Medial ridge of the distal trochlea of the talus; (26) Lateral ridge of proximal trochlea of the talus; (27) Lateral ridge of distal trochlea of the talus.

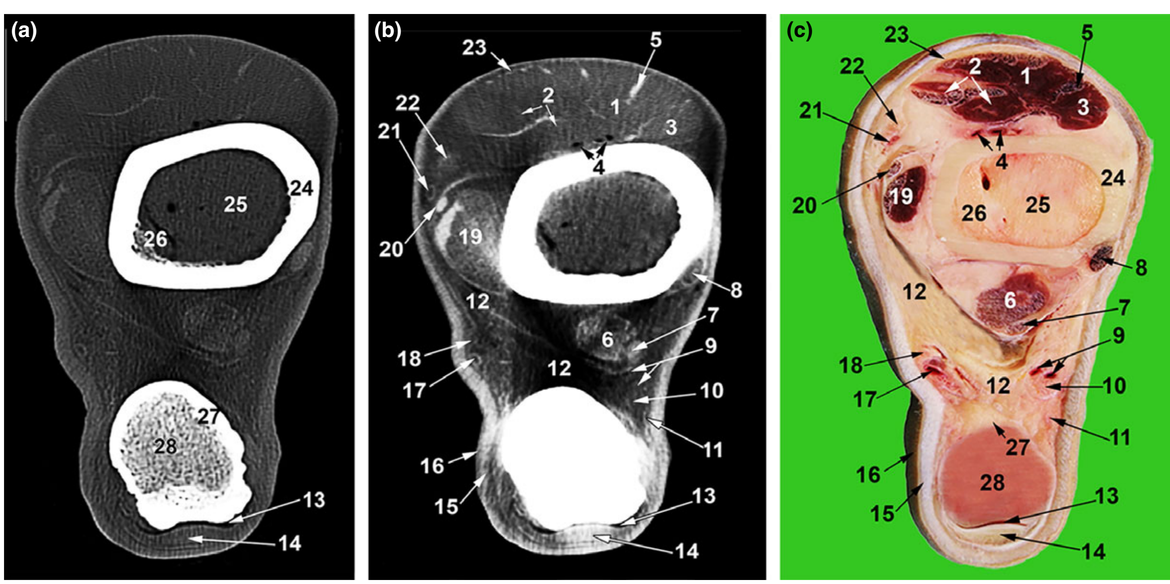

Fig. 2. Transverse CT scans at the level of the proximal calcaneal tuber (level 1 as indicated in Fig. 1): bone window (a), soft tissue window (b) and their corresponding transverse cryosection (c) of a clinically normal bovine tarsus. The images are oriented with the lateral aspect to the left and the dorsal aspect to the top: (1) M. fibularis tertius; (2) M. long digital extensor; (3) M. tibialis cranialis; (4) Cranial tibial A. and V.; (5) Intermuscular septum; (6) M. lateral digital flexor; (7) M. tibialis caudalis; (8) M. medial digital flexor; (9) Caudal branches of saphenous A. and medial saphenous V.; (10) Tibial N.; (11) Calcaneal branch of saphenous A. (caudal branch); (12) Deep lamina of crural fascia; (13) Subtendinous calcaneal bursa of the superficial digital flexor muscle; (14) Superficial digital flexor tendon; (15) Subcutis; (16) Cutis; (17) Caudal branch of lateral saphenous V.; (18) Caudal cutaneous sural N.; (19) M. lateral digital extensor; (20) Fibularis longus tendon; (21) Cranial branch of lateral saphenous V.; (22) Cutaneous branch of superficial fibular N.; (23) Crural extensor retinaculum; (24) Compact bone of tibia; (25) Bone marrow of tibia; (26) Cancellous bone of tibia; (27) Cortical bone of calcaneus; (28) Cancellous bone of calcaneal tuber.

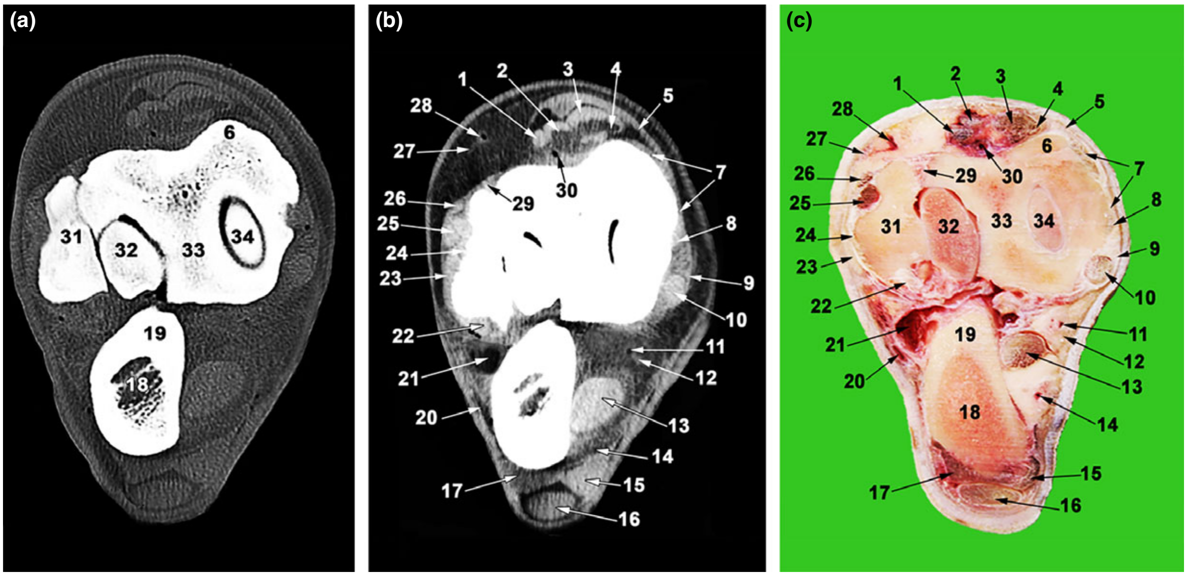

Fig. 3. Transverse CT scans at the level of the tibial cochlea (level 2 as indicated in Fig. 1): bone window (a), soft tissue window (b) and their corresponding transverse cryosection (c) of a clinically normal bovine tarsus. The images are oriented with the lateral aspect to the left and the dorsal aspect to the top: (1) M. long digital extensor (tendon of lateral part); (2) M. long digital extensor (tendon of medial part); (3) Fibularis tertius tendon; (4) Cranial tibial tendon; (5) Crural fascia; (6) Cranial end of tibial cochlea; (7) Long part of the medial collateral tarsal ligament; (8) Pars tibiotalaris of the short medial collateral tarsal ligament; (9) Tendon sheath of the corresponding muscle; (10) Medial digital flexor tendon; (11) Medial malleolar branch of the saphenous A. (Caudal branch); (12) Medial plantar N.; (13) Common tendon of the lateral digital flexor and caudal tibial muscles; (14) Saphenous A. and medial saphenous V. (caudal branches); (15) Long plantar ligament (medial part); (16) Superficial digital flexor tendon; (17) Long plantar ligament (lateral part); (18) Cancellous bone of calcaneus; (19) Cortical bone of calcaneus; (20) Caudal branch of the lateral saphenous V.; (21) Plantarolateral recess of the tarsocrural joint; (22) Caudal tibiofibular ligament; (23) Long part of the lateral collateral tarsal ligament; (24) Pars calcaneofibularis of the short lateral collateral tarsal ligament; (25) M. lateral digital extensor; (26) Fibularis longus tendon; (27) Caudal cutaneous sural N.; (28) Cranial branch of the lateral saphenous V.; (29) Cranial tibiofibular ligament; (30) Dorsal pedal A. and V.; (31) Malleolar bone; (32) Lateral part of the proximal trochlea of the talus; (33) Tibial sagittal ridge; (34) Medial part of the proximal trochlea of the talus.

of the clinically normal bovine tarsus via comparison of CT images with gross specimens.

Materials and Methods

Twelve pelvic limbs from six adult bovine cadavers (age range: 3 – 12 years) were used in the study. Cows were euthanized for reasons unrelated to musculoskeletal disorders and limbs were disarticulated at the stifle joint. Limbs were inspected, palpated and radiographed (dorsoplantar and lateromedial planes); no gross or radiographic abnormalities were identified. The CT examination was conducted using 16-detector row helical scanner (Philips Mx8000 IDT 16-slice helical CT scanner; Philips, GmbH, Hamburg, Germany). Limbs were extended and placed on their lateral aspect so that the long axis of the limb was parallel to the long axis of the CT table. A scout image (120 kV and 50 mA) was obtained to ensure symmetry in positioning and inclusion of the entire region of interest. The limbs were scanned in helical fashion in a proximal to distal direction (starting at a level proximal to the calcaneal tuber and continued distally towards the proximal metatarsus). The acquisition settings were 120 kV, 400 mA, slice thickness of 1.5 mm, slice increment of 0.6 mm, rotation time of 1 second, pitch of 0.635, scan field of view of 22 cm and matrix size of 512 × 512 pixels. The obtained transverse CT images were reconstructed into sagittal and dorsal slices from the distal end of tibia to the proximal extremity of the metatarsus.

The limbs were frozen at −20° C maintaining the same position as in the CT study for at least 48 hours and sectioned in transverse, sagittal and dorsal planes via an electric band saw. Sections began strictly following the imaging protocol; however, each section was approximately 10 mm thick. Each slice was rinsed with water, numbered and photographed. The anatomic sections were inspected. The bony and soft tissue structures were identified and subsequently located on the corresponding CT images based on shape, size, location and tissue density characteristics. Differentiation and identification was performed with the aid of anatomic references (Dyce et al.,

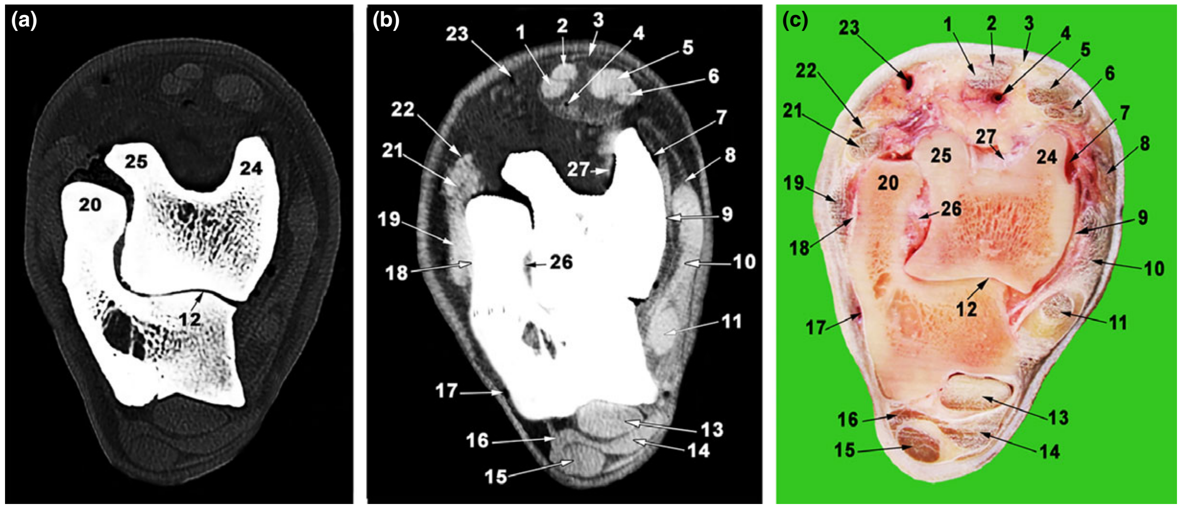

Fig. 4. Transverse CT scans at the level of the talocalcaneal joint (level 3 as indicated in Fig. 1): bone window (a), soft tissue window (b) and their corresponding transverse cryosection (c) of a clinically normal bovine tarsus. The images are oriented with the lateral aspect to the left and the dorsal aspect to the top: (1) M. long digital extensor (tendon of lateral part); (2) M. long digital extensor (tendon of medial part); (3) Crural extensor retinaculum; (4) Dorsal pedal A. and V.; (5) Fibularis tertius tendon; (6) Cranial tibial tendon; (7) Dorsomedial pouch of tarsocrural joint; (8) Talocentro-distometatarsal ligament; (9) Pars tibiocalcanea of the short medial collateral tarsal ligament; (10) Long part of the medial collateral tarsal ligament; (11) Medial digital flexor tendon; (12) Talocalcaneal joint; (13) Common tendon of the lateral digital flexor and caudal tibial muscles; (14) Long plantar ligament (medial part); (15) Superficial digital flexor tendon; (16) Long plantar ligament (lateral part); (17) Caudal branch of the lateral saphenous V.; (18) Pars calcaneofibularis of the short lateral collateral tarsal ligament; (19) Long part of the lateral collateral tarsal ligament; (20) Lateral part of calcaneal base; (21) Lateral digital extensor tendon; (22) Fibularis longus tendon; (23) Cranial branch of the lateral saphenous V.; (24) Medial part of the proximal trochlea of the talus; (25) Lateral part of the proximal trochlea of the talus; (26) Lateral talocalcaneal ligament; (27) Dorsal tarsal ligament.

2010; Budras et al., 2011) and labelled according to the 'Nomina Anatomica Veterinaria, 2012'.

Results

Clinically relevant anatomic structures were identified and formatted as labelled sequential triples of two CT scans (bone and soft tissue windows) and their corresponding cryosection. The bone structures included the tibial cochlea, malleolar bone, calcaneus, talus with its trochlear ridges, fused central and 4th tarsal bones (centroquartal bone), 1st tarsal bone, fused 2nd and 3rd tarsal bones, 3rd and 4th metatarsal bones and the sesamoid metatarsal bone (Fig. 1). By use of the bone window settings, tarsal bones had smooth outline and homogenous contours. The entire images had excellent delineation between the cortex and medulla of bones, and the trabecular pattern was clearly depicted. The tarsocrural, talocalcaneocentral, centrodistal and tarsometatarsal joints together with the inter-tarsal bone relations were evaluated (Figs 2–11).

The soft tissue structures involved the following: the regional muscles (distal end of gastrocnemius, fibularis tertius, long digital extensor, cranial tibial, fibularis longus, lateral digital extensor, lateral digital flexor, caudal tibial, medial digital flexor, short digital extensor and middle inter-osseous) with their tendons, the superficial digital flexor tendon (SDFT), joint capsules, bursae and the collateral, proximal and distal tarsal and tarsometatarsal ligaments (Figs 2–11).

By use of the soft tissue window settings, soft tissue structures showed variable shades of grey. Regional muscles (compared to their tendons), musculotendinous structures (junction between the muscle and its tendon) and tendons were recognized as hypo-attenuated, heterogeneous and hyperattenuated structures, respectively, and the synovial fluid was the lowest attenuated structure (Figs 2–7). The tendons of the fibularis tertius and cranial tibial muscles terminated on the large metatarsal bones, while the long digital extensor tendon proceeded over the lateral aspect of the tarsus (Fig. 7). The fibularis longus crossed the plantar surface of the tarsus and terminated on the 1st tarsal and centroquartal bones (Fig. 6).

The caudal tibial and lateral digital flexor tendons united at the level of the tarsocrural joint forming a common tendon (Fig. 3). The latter united with the medial digital flexor tendon, at the level of the distal inter-tarsal joint, to form the deep digital flexor tendon (Fig. 6). The SDFT was evident plantar to the calcaneus as a well-defined hyperattenuated linear structure beneath the skin

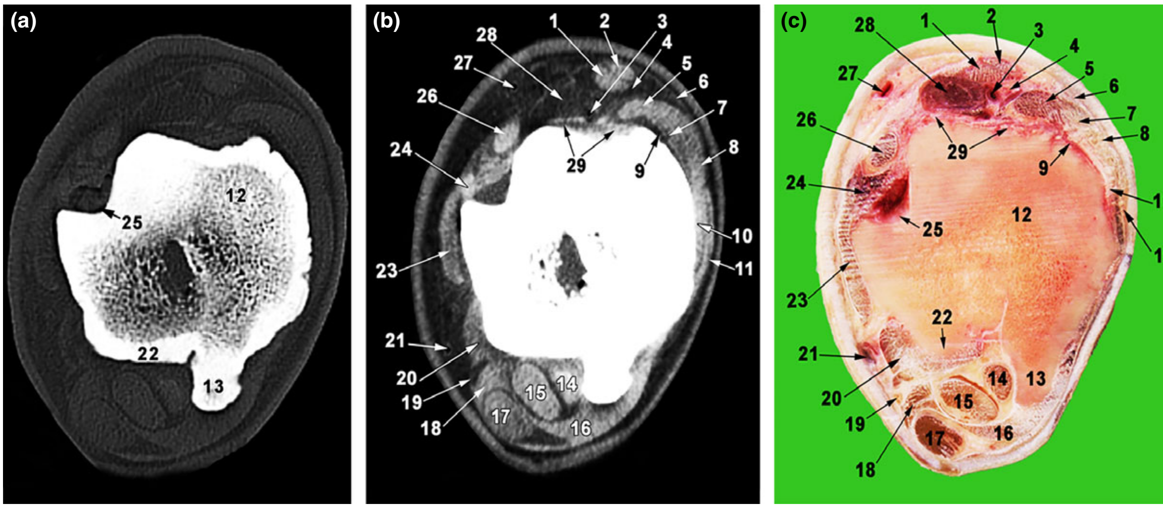

Fig. 5. Transverse CT scans at the level of the centroquartal bone (level 4 as indicated in Fig. 1): bonewindow (a), soft tissue window (b) and corresponding transverse cryosection (c) of a clinically normal bovine tarsus. The images are oriented with the lateral aspect to the left and the dorsal aspect to the top: (1) M. long digital extensor (tendon of lateral part); (2) M. long digital extensor (tendon of medial part); (3) Dorsal pedal A. and V.; (4) Deep fibular N.; (5) Fibularis tertius tendon; (6) Metatarsal extensor retinaculum; (7) Cranial tibial tendon; (8) Talocentrodistometatarsal ligament; (9) Subtendinous bursa of the cranial tibial tendon; (10) Pars tibiocentralis of the short medial collateral tarsal ligament; (11) Long part of the medial collateral tarsal ligament; (12) Centroquartal bone; (13) Plantomedial crest of the centroquartal bone; (14) Medial digital flexor tendon; (15) Common tendon of the lateral digital flexor and caudal tibial muscles; (16) Long plantar ligament (medial part); (17) Superficial digital flexor tendon; (18) Long plantar ligament (lateral part); (19) Lateral plantar N.; (20) Plantar calcaneocentral ligament; (21) Lateral plantar A. and V.; (22) Plantolateral crest of the centroquartal bone; (23) Long lateral collateral tarsal ligament; (24); Fibularis longus tendon; (25) Lateral groove of centroquartal bone; (26) Lateral digital extensor tendon; (27) Cranial branch of the lateral saphenous V.; (28) Short digital extensor muscle; (29) Dorsal tarsal ligament.

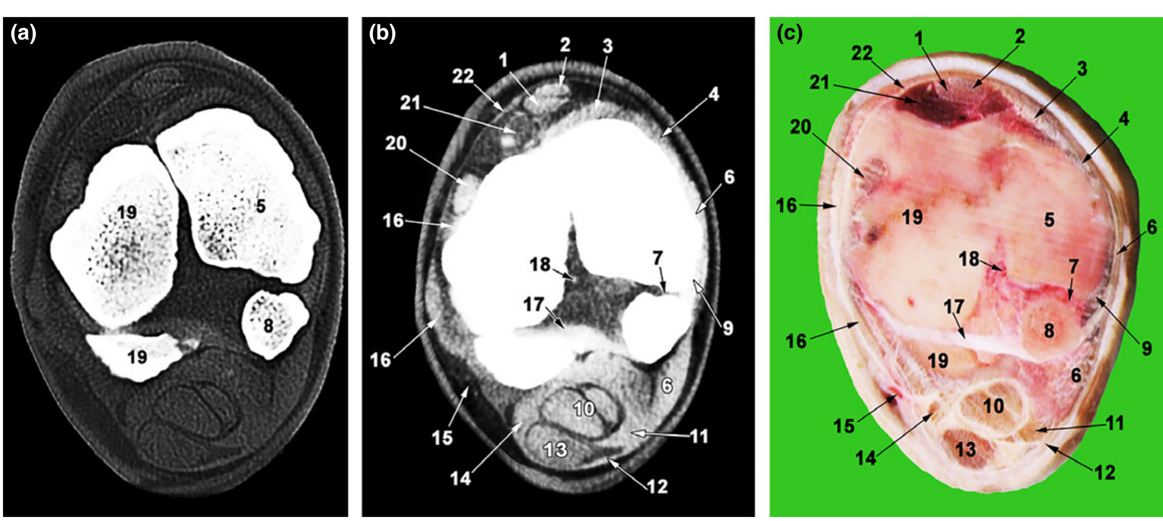

Fig. 6. Transverse CT scans at the level of the distal row of tarsal bones (level 5 as indicated in Fig. 1): bone window (a), soft tissue window (b) and corresponding transverse cryosection (c) of a clinically normal bovine tarsus. The images are oriented with the lateral aspect to the left and the dorsal aspect to the top: (1) M. long digital extensor (tendon of lateral part); (2) M. long digital extensor (tendon of medial part); (3) Fibularis tertius tendon; (4) Talocentrodistometatarsal ligament; (5) Fused 2nd and 3rd tarsal bones; (6) Long part of the medial collateral tarsal ligament; (7) Cranial tibial tendon; (8) 1st tarsal bone; (9) Pars tibiocentralis of the short medial collateral tarsal ligament; (10) Deep digital flexor tendon; (11) Long plantar ligament (medial part); (12) Tarsal flexor retinaculum; (13) Superficial digital flexor tendon; (14) Long plantar ligament (lateral part); (15) Caudal branches of the lateral saphenous V. and lateral plantar V.; (16) Long part of the lateral collateral tarsal ligament; (17) Fibularis longus tendon; (18) Perforating tarsal A.; (19) Centroquartal bone; (20) Lateral digital extensor tendon; (21) Short digital extensor muscle; (22) Metatarsal extensor retinaculum.

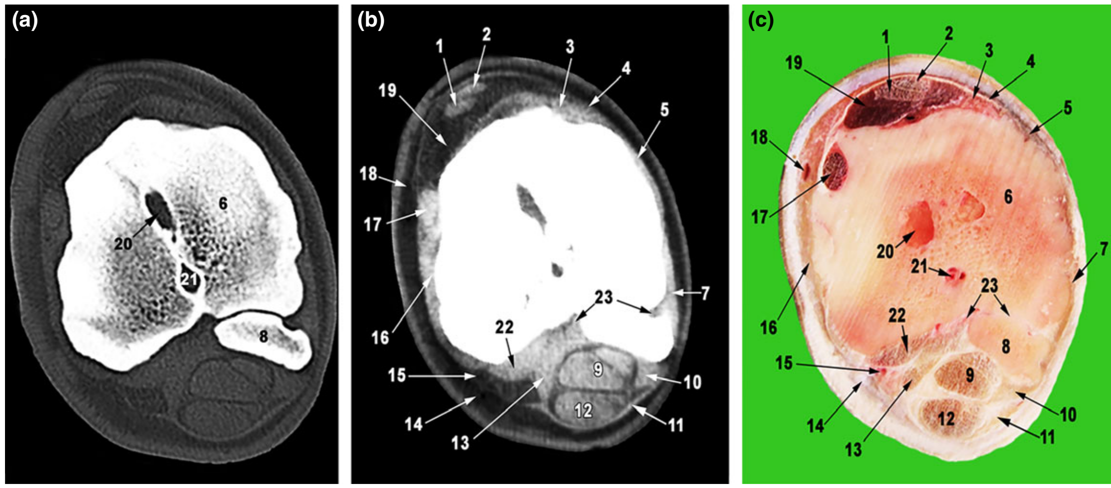

Fig. 7. Transverse CT scans at the level of the tarsometatarsal joint (level 6 as indicated in Fig. 1): bone window (a), soft tissue window (b) and corresponding transverse cryosection (c) of a clinically normal bovine tarsus. The images are oriented with the lateral aspect to the left and the dorsal aspect to the top: (1) M. long digital extensor (tendon of lateral part); (2) M. long digital extensor (tendon of medial part); (3) Fibularis tertius tendon; (4) Metatarsal extensor retinaculum; (5) Dorsal tarsal ligament; (6) 3rd and 4th metatarsal bones; (7) Long part of the medial collateral tarsal ligament; (8) Sesamoid metatarsal bone; (9) Deep digital flexor tendon; (10) Long plantar ligament (medial part); (11) Tarsal flexor retinaculum; (12) Superficial digital flexor tendon; (13) Long plantar ligament (lateral part); (14) Lateral plantar N.; (15) Caudal branches of the lateral saphenous V. and lateral plantar V.; (16) Long part of the lateral collateral tarsal ligament; (17) Lateral digital extensor tendon; (18) Cranial branch of the lateral saphenous V.; (19) Short digital extensor muscle; (20) Metatarsal medullary cavity; (21) Perforating tarsal A.; (22) Plantar calcaneocentral ligament; (23) Sesamoidometatarsal ligament.

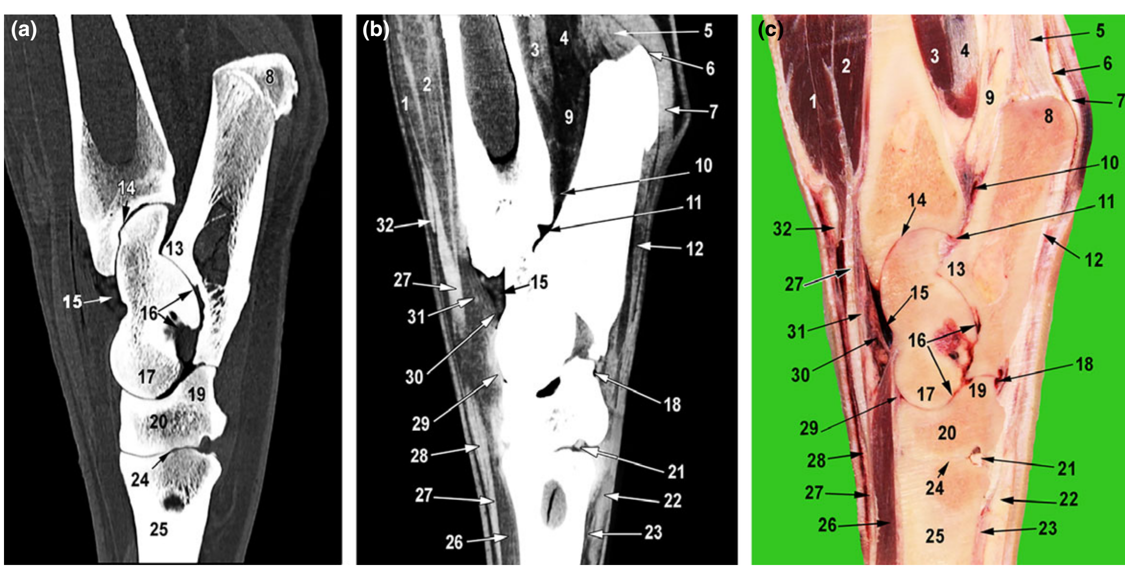

Fig. 8. Sagittal CT scans at the level of the lateral aspect of the talocalcaneal joint and lateral trochlear ridge of the talus (level 7 as indicated in Fig. 1): bone window (a), soft tissue window (b) and corresponding transverse cryosection (c) of a clinically normal bovine tarsus. The images are oriented with the dorsal aspect to the left and the proximal aspect to the top: (1) M. fibularis tertius; (2) M. long digital extensor; (3) Lateral digital flexor tendon; (4) M. tibialis caudalis; (5) Tendon of the lateral head of the gastrocnemius muscle; (6); Subtendinous calcaneal bursa of the superficial digital flexor muscle; (7) Superficial digital flexor tendon; (8) Calcaneal tuber; (9) Deep crural fascia; (10) Joint capsule, plantar strengthening; (11) Plantarolateral recess of the tarsocrural joint; (12) Long plantar ligament (lateral part); (13) Lateral part of the calcaneal base; (14) Tarsocrural joint; (15) Dorsal recess of the tarsocrural joint; (16) Talocalcaneocentral joint; (17) Distal trochlea of the talus; (18) Calcaneal branch of the saphenous A. (caudal branch); (19) Proximal process of the centroquartal bone; (20) Centroquartal bone; (21) Fibularis longus tendon; (22) Deep digital flexor tendon; (23) M. Interosseus medius; (24) Tarsometatarsal joint; (25) 3rd and 4th metatarsal bones; (26) M. short digital extensor; (27) M. long digital extensor (tendon of lateral part); (28) Metatarsal extensor retinaculum; (29) Fibularis tertius tendon; (30) Tarsocrural joint capsule, dorsal strengthening; (31) Cranial tibial tendon; (32) Crural extensor retinaculum.

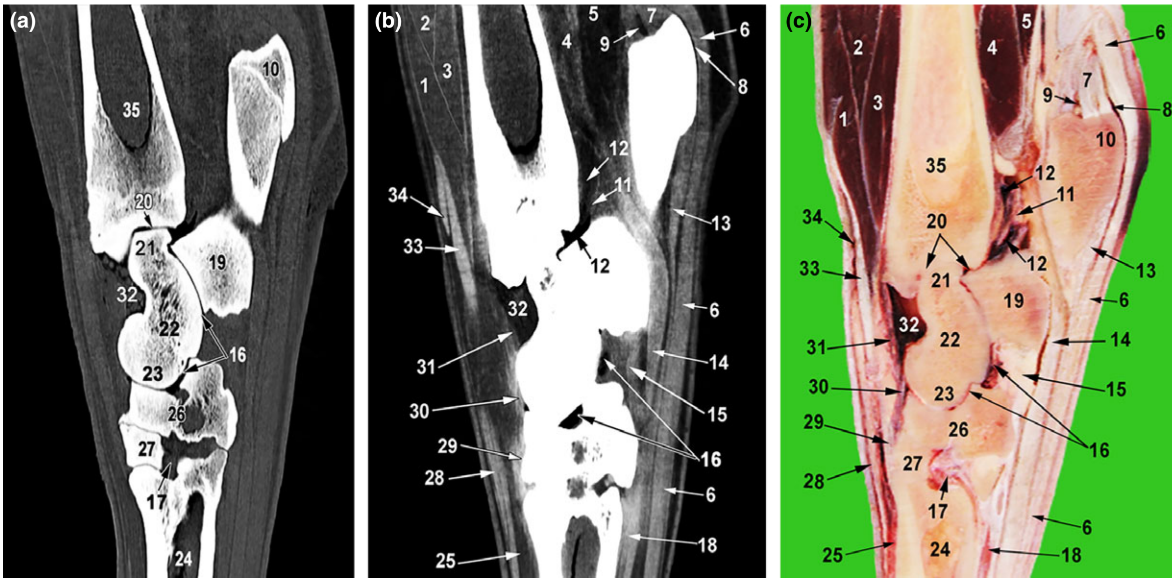

Fig. 9. Sagittal CT scans at the level of the medial aspect of the talocalcaneal joint and medial trochlear ridge of the talus (level 8 as indicated in Fig. 1): bone window (a), soft tissue window (b) and corresponding transverse cryosection (c) of a clinically normal bovine tarsus. The images are oriented with the dorsal aspect to the left and the proximal aspect to the top: (1) M. fibularis tertius; (2) M. long digital extensor; (3) M. tibialis cranialis; (4) Lateral digital flexor tendon; (5) M. tibialis caudalis; (6) Superficial digital flexor tendon; (7) Tendon of the medial head of the gastrocnemius muscle; (8) Subtendinous calcaneal bursa of the superficial digital flexor muscle; (9) Tendinous calcaneal bursa; (10) Calcaneal tuber; (11) Tarsocrural joint capsule, plantar strengthening; (12) Plantar recess of the tarsocrural joint; (13) Long plantar ligament (medial part); (14) Deep digital flexor tendon; (15) Plantar calcaneocentral ligament; (16) Talocalcaneocentral joint; (17) Tarsometatarsal joint; (18) M. interosseus medius; (19) Sustentaculum tali; (20) Tarsocrural joint; (21) Proximal trochlea of the talus; (22) Talus; (23) Distal trochlea of the talus; (24) Metatarsal medullary cavity; (25) M. short digital extensor; (26) Centroquartal bone; (27) Fused 2nd and 3rd tarsal bones; (28) Metatarsal extensor retinaculum; (29) Cranial tibial tendon; (30) Talocentrodistometatarsal ligament; (31) Tarsocrural joint capsule, dorsal strengthening; (32) Dorsal recess of the tarsocrural joint; (33) Fibularis tertius tendon; (34) Crural extensor retinaculum; (35) Tibia, medullary cavity.

(Figs 2–7). It continued distally on the plantar aspect of the tarsus as an ovoid hyperattenuated structure.

The ligaments of the tarsus were recognized as hyperattenuated linear structures (Figs 2–11). The collateral ligaments were medial and lateral collateral ligaments. Each collateral ligament had a long superficial part and short deep part(s). The short medial collateral ligaments were the pars tibiotalaris, pars tibiocalcanea and the pars tibiocentralis. The short lateral collateral ligament was represented by the pars calcaneofibularis. The proximal tarsal ligaments included the lateral and plantar talocalcaneal ligaments. The distal tarsal ligaments were the dorsal, plantar and inter-osseous ligaments. The medial and lateral limbs of the long plantar ligament were depicted along the plantar aspect of the tarsus. The tarsometatarsal ligaments included several small structures and the most prominent and clinically import ligament was the talocentrodistometatarsal ligament.

Discussion

The present study was performed to provide a detailed reference CT images with corresponding anatomic sections of the bovine tarsus in various planes. The images afforded valuable information on bone and soft tissue structures that should enhance the clinical use of CT in the diagnosis of various bovine tarsal pathologies. CT images were obtained in transverse, sagittal and dorsal planes. The sagittal and dorsal reconstructions were valuable and complementary to the transverse plane for consistent evaluation of the clinically relevant structures of the bovine tarsus. The sagittal plane was indispensable for evaluation of bone contours, the dorsal plane was valuable in examination of the collateral ligaments, and both were beneficial for assessment of the tarsal joint articulations as well. This is in agreement with the previous studies of the equine tarsus (Blaik et al., 2000; Latorre et al., 2006; Raes et al., 2011).

In the current study, all bone structures were recognized on transverse, sagittal and dorsal plane scans. The regional muscles were clearly identified and delineated. The insertion of the cranial tibial muscle on the large metatarsal bones was clearly recognized on the sagittal slices, while on the transverse sections it was difficult to differentiate its tendon from the dorsal tarsal ligament, as they were similar in density and closely connected

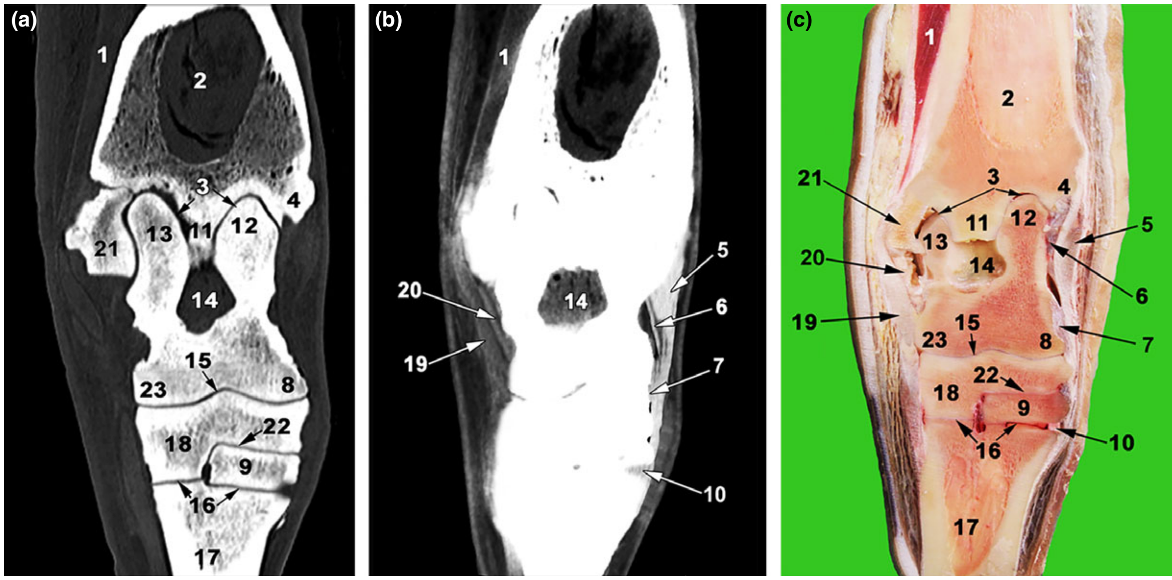

Fig. 10. Dorsal CT scans at the level of the tibial malleoli (level 9 as indicated in Fig. 1): bone window (a), soft tissue window (b) and corresponding transverse cryosection (c) of a clinically normal bovine tarsus. The images are oriented with the lateral aspect to the left and the proximal aspect to the top: (1) M. lateral digital flexor; (2) Tibia, medullary cavity; (3) Tarsocrural joint; (4) Medial malleolus; (5) Long part of the medial collateral tarsal ligament; (6) Pars tibiotalaris of the short medial collateral tarsal ligament; (7) Talocentrodistometatarsal ligament; (8) Medial part of the distal trochlea of the talus; (9) Fused 2nd and 3rd tarsal bones; (10) Tarsometatarsal ligament; (11) Tibial sagittal ridge; (12) Medial part of the proximal trochlea of the talus; (13) Lateral part of the proximal trochlea of the talus; (14) Tarsal sinus; (15) Talocalcaneocentral joint; (16) Tarsometatarsal joint; (17) 3rd and 4th metatarsal bones; (18) Centroquartal bone; (19) Long part of the lateral collateral tarsal ligament; (20) Pars calcaneofibularis of the short lateral collateral tarsal ligament; (21) Malleolar bone; (22) Centrodistal joint; (23) Medial part of the distal trochlea of the talus.

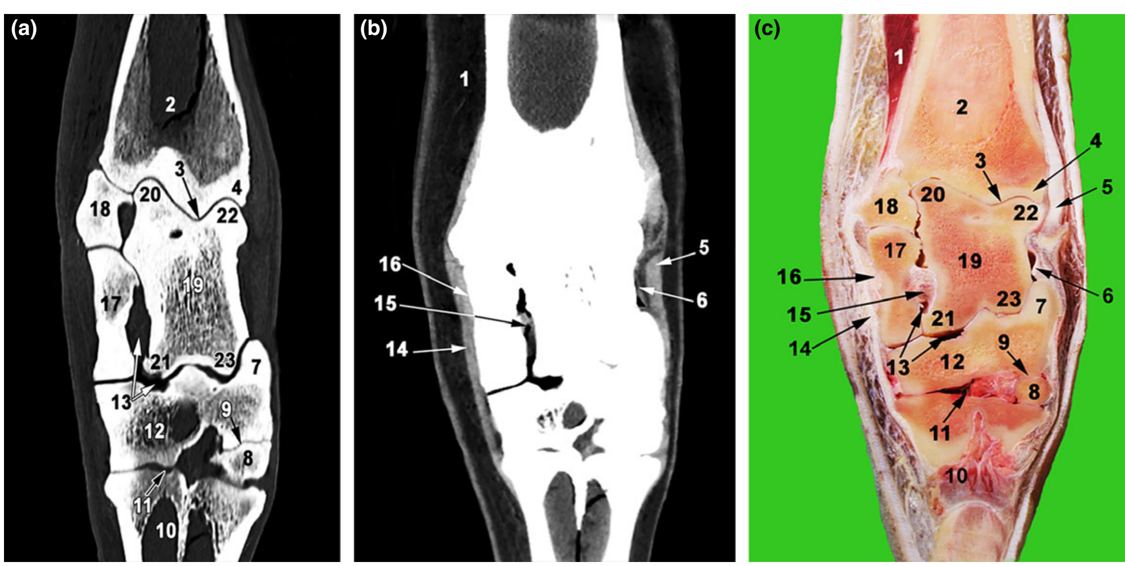

Fig. 11. Dorsal CT scans at the level of the lateral part of the calcaneal base (level 10 as indicated in Fig. 1): bone window (a), soft tissue window (b) and corresponding transverse cryosection (c) of a clinically normal bovine tarsus. The images are oriented with the lateral aspect to the left and the proximal aspect to the top: (1) M. lateral digital flexor; (2) Tibia, medullary cavity; (3) Tarsocrural joint; (4) Medial malleolus; (5) Long part of the medial collateral tarsal ligament; (6) Pars tibiocentralis of the short medial collateral tarsal ligament; (7) Proximal process of the centroquartal bone; (8) Fused 2nd and 3rd tarsal bones; (9) Centrodistal joint; (10) 3rd and 4th metatarsal bones; (11) Tarsometatarsal joint; (12) Centroquartal bone; (13) talocalcaneocentral joint; (14) Long part of the lateral collateral tarsal ligament; (15) Lateral talocalcaneal ligament; (16) Pars calcanofibularis of the short lateral collateral tarsal ligament; (17) Calcaneus; (18) Malleolar bone; (19) Talus; (20) Lateral part of the proximal trochlea of the talus; (21) Lateral part of the distal trochlea of the talus; (22) Medial part of the proximal trochlea of the talus; (23) Medial part of the distal trochlea of the talus.

with each other and the surrounding fascia. The limbs of the long plantar ligament were well identified along the plantar aspect of the tarsus. The collateral ligaments were clearly delineated and the long lateral and medial collateral ligaments were differentiated from the short deep parts on the ipsilateral aspect of the tarsal joint. Similar findings were reported in equine (Vanderperren et al., 2008; Raes et al., 2011; Van der Vekens et al., 2011) and canine (Gielen et al., 2001). However, in equine tarsus (Peterson and Bowman, 1988), the subdivisions of the deep collateral ligaments were not visible, while in carpal and fetlock joints (Kaser-Hotz et al., 1994; Latorre et al., 2006) differentiation between the superficial and deep parts of the collateral ligaments was impossible.

CT imaging is a non-invasive diagnostic technique that offers considerable advantages over the traditional diagnostic modalities. Compared to radiography and ultrasonography, CT provides a highly detailed cross-sectional image and the possibility of a three-dimensional imaging obtained by reconstruction without superimposition of the bony structures (van Weeren and Firth, 2008). With the use of multislice scanners, the loss of image quality after reconstruction in the orthogonal planes is substantially reduced. Images in the current study were obtained via a multirow detector helical CT scanner that possesses a high image quality and a considerable enhanced resolution of small structures (Lee et al., 2009), compared with the conventional axial. Improvements were attributed to the thinner collimation, faster scanning, higher spatial resolution, decrease in noise and larger number of images generated during the same scanning time (Lee et al., 2009).

The use of CT in bovine orthopaedics is relatively confined to advanced veterinary clinics due to high cost and the need for general anaesthesia. Another limitation of the use of CT in bovine practice is that the diameter of the gantry is not large enough to allow the passage of the whole body of the animal. However, it is possible to obtain a CT scan of the entire body (Lubbers et al., 2007) of calves and the head (Van Biervliet et al., 2004) and limbs (Raji et al., 2008) of cattle. Despite its cost, the use of CT should be considered for economically valuable cattle for achieving a comprehensive diagnosis and planning of a surgical intervention (Kofler et al., 2014). Delayed diagnosis and/or repeated treatments without a correct diagnosis can lead to economic losses. Therefore, the cost savings per animal may well be beneficial if early diagnosis is achieved through the use of CT (Lee et al., 2009).

In the current study, computed tomography allowed a full assessment of the bovine tarsus and proved that CT is a valuable imaging technique for evaluation of both soft and bony structures. This study showed that the use of CT during routine examination of cattle may play an important role in providing additional information to assist diagnosis and the images provided in this study can serve as a CT reference for the clinically normal bovine tarsus.

References

Becker, M., C. Heun, G. Tsousis, and H. Bollwein, 2011: Application of computed tomography for the evaluation of obstetrically relevant measurements in German Holstein-Friesian calves. Theriogenology. **75**, 1052–1056.

Blaik, M. A., R. R. Hanson, and S. A. Kincaid, 2000: Low-field magnetic resonance imaging of the equine tarsus: normal anatomy. Vet. Radiol. Ultrasound. **41**, 131–141.

Budras, K. D., R. E. Habel, C. K. W. Mülling, P. R. Greenough, J. G. Gisela, R. Richter, and D. Starke, 2011: Bovine Anatomy: An Illustrated Text. Hannover, Germany: Verlag and Druckered.

Dyce, K. M., W. O. Sack, and C. J. G. Wensing, 2010: Textbook of Veterinary Anatomy. Missouri: Saunders, Elsevier.

El-Khodery, S., K. Yamada, D. Aoki, K. Kamio, M. Kishimoto, J. Shimizu, Y. Kobayashi, M. Ishii, H. Inokuma, S. Yamauchi, and T. Matsui, 2008: Brain abscess in a Japanese black calf: utility of computed tomography (CT). J. Vet. Med. Sci. **70**, 727–730.

Frame, E. M., H. Gufler, W. Henninger, and J. Gasteiner, 2000: Diagnosis of atrophic rhinitis in a Simmental heifer by computed tomography. Vet. Rec. **146**, 558–560.

Frederick, J. D., R. J. Mackay, M. D. Winter, and W. L. Castleman, 2009: Vertebral osteomyelitis with abscessation in a Holstein calf. Vet. Rec. **164**, 723–724.

Gielen, I. M., L. M. De Rycke, H. J. van Bree, and P. J. Simoens, 2001: Computed tomography of the tarsal joint in clinically normal dogs. Am. J. Vet. Res. **62**, 1911–1915.

Hagag, U., W. Brehm, R. O. Ramadan, A. Al Mubarak, A. El Nahas, and K. Gerlach, 2013: Computed tomography and cross-sectional anatomy of the normal dromedary camel tarsus (one humped camel). Anat. Histol. Embryol. **42**, 266–274.

Hernandez, J., J. K. Shearer, and D. W. Webb, 2002: Effect of lameness on milk yield in dairy cows. J. Am. Vet. Med. Assoc. **220**, 640–644.

Kaser-Hotz, B., S. Sartoretti-Schefer, and R. Weiss, 1994: Computed tomography and magnetic resonance imaging of the normal equine carpus. Vet. Radiol. Ultrasound. **35**, 457–461.

Kofler, J., U. Geissbühler, and A. Steiner, 2014: Diagnostic imaging in bovine orthopedics. Vet. Clin. North Am. Food Anim. Pract. **30**, 11–53.

Latorre, R., A. Arencibia, F. Gil, M. Rivero, R. W. Henry, G. Ramírez, and J. M. Váquez, 2006: Correlation of magnetic resonance images with anatomic features of the equine tarsus. Am. J. Vet. Res. **67**, 756–761.

Lee, K., K. Yamada, R. Tsuneda, M. Kishimoto, J. Shimizu, Y. Kobayashi, H. Furuoka, T. Matsui, N. Sasaki, M. Ishii, H. Inokuma, T. Iwasaki, and Y. Miyake, 2009: Clinical experience of using multidetector-row CT for the diagnosis of disorders in cattle. Vet. Rec. **165**, 559–562.

Lee, K. J., M. Kishimoto, J. Shimizu, Y. Kobayashi, K. Matsumoto, N. Sasaki, M. Ishii, H. Inokuma, T. Iwasaki, Y. Miyake, and K. Yamada, 2011: Use of contrast-enhanced CT in the diagnosis of abscesses in cattle. J. Vet. Med. Sci. **73**, 113–115.

Lubbers, B. V., M. D. Apley, J. F. Coetzee, D. A. Mosier, D. S. Biller, D. E. Mason, and P. N. Henao-Guerrero, 2007: Use of computed tomography to evaluate pathologic changes in the lungs of calves with experimentally induced respiratory tract disease. Am. J. Vet. Res. **68**, 1259–1264.

Nelson, D. R., and S. K. Kneller, 1985: Treatment of proximal hind-limb lameness in cattle. Vet. Clin. North Am. Food Ani. Pract. **1**, 153–173.

Nomina Anatomica Veterinaria, 2012: Prepared by the International Committee on veterinary Gross Anatomical Nomenclature and authorized by the General Assembly of the World Association of Veterinary Anatomists. Knoxville, TN (U.S.A), Hannover (Germany), Columbia, MO (USA), Ghent (Belgium), Sapparo (Japan): Published by the Editorial Committee. pp. 14–48.

Nuss, K., C. Schnetzler, R. Hagen, P. R. Schwarz, and A. Kircher, 2011: Klinische Anwendung der Computertomographie beim Rind. Tierarztl. Prax. Ausg. G Grosstiere Nutztiere. **39**, 317–324.

Peterson, R. P., and K. F. Bowman, 1988: Computed tomography of the distal extremity of the horse. Vet. Rad. **29**, 147–156.

Raes, E. V., E. H. J. Bergman, H. van der Veen, K. Vanderperren, E. Van der Vekens, and J. H. Saunders, 2011: Comparison of cross-sectional anatomy and computed tomography of the tarsus in horses. Am. J. Vet. Res. **72**, 1209–1221.

Raji, A., K. Sardari, and H. Mohammadi, 2008: Normal cross-sectional anatomy of the bovine digit: comparison of computed tomography and limb anatomy. Anat. Hist. Embryol. **37**, 188–191.

Tomlinson, J. E., W. R. Redding, and C. Berry, 2003: Computed tomographic anatomy of the equine tarsus. Vet. Radiol. Ultrasound. **44**, 174–178.

Van Biervliet, J., G. A. Perkins, B. Woodie, A. Pelligrini-Massini, T. J. Divers, and A. de Lahunta, 2004: Clinical signs, computed tomographic imaging, and management of chronic otitis media/interna in dairy calves. J. Vet. Int. Med. **18**, 907–910.

Van der Vekens, E., E. H. Bergman, H. van der Veen, K. Vanderperren, E. V. Raes, S. M. Puchalski, H. J. van Bree, and J. H. Saunders, 2011: computed tomographic anatomy of the equine stifle joint. Am. J. Vet. Res. **72**, 512–521.

Vanderperren, K., B. Ghaye, F. R. Snaps, and J. H. Saunders, 2008: Evaluation of computed tomographic anatomy of the equine metacarpophalangeal joint. Am. J. Vet. Res. **69**, 631–638.

van Weeren, P. R., and E. C. Firth, 2008: Future tools for early diagnosis and monitoring of musculoskeletal injury: biomarkers and ct. Vet. Clin. North Am. Equine Pract. **24**, 153–175.